CATALYTIC AGENT DEGRADATION ON OXIDE FILMS AND IN MICROHETEROGENEOUS SOLUTION SYSTEMS

Seventh Interim and Final Report

by

Michael Grätzel, Ph.D.
Professor of Chemistry

February 18, 1993

United States Army

European Research Office of the U.S. Army
London, England

CONTRACT NO. DAJA45-90-C-0007

Michael Grätzel, Ph.D.
Professor of Chemistry
Ecole Polytechnique Fédérale
CH-1015 Lausanne, Switzerland

"Approved for Public Release, Distribution Unlimited"

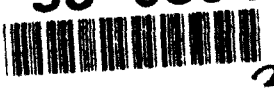

Studies over the period January 1990 - January 1993 of grant No. **DAJA45-90-C-0007** centered principally on investigations of the thermal and/or photolytic degradation of toxic compounds in aqueous solutions containing hydrogen peroxide (as sacrificial oxidant) and Fe (III) salts as catalytic agents.

Extensive investigations were carried out on the simulants 4-NPDEP (paraoxon, 4-nitrophenyl diethyl phosphate), 4-NPIPP (4-nitrophenyl isopropyl phenyl phosphinate), DEP (diethyl ethyl phosphonate), NOX (nitro-o-oxylene), TSPAP (thiosulfuric acid-S- (2-diisopropyl amino ethyl)-O-phenylester, 4-NP (4-nitrophenol), 4-CP (4-chlorophenol), and DBP (diethyl benzylphosponate). Both DBP and KHP (potassium hydrogen phthalate) were used as model compounds in attempts to elucidate the mechanism of the photocatalytic reaction in presence of Fe (III) salts.

The stoichiometric relationships for these oxidative degradation reactions are expressed in equations **1-8**.

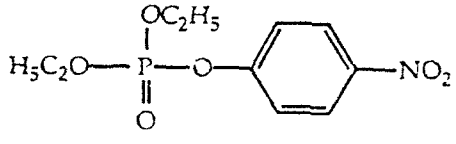

4-NPDEP

$$+ \; 13\,O_2 \longrightarrow 10\,CO_2 + H_3PO_4 + HNO_3 + 5H_2O \qquad (1)$$

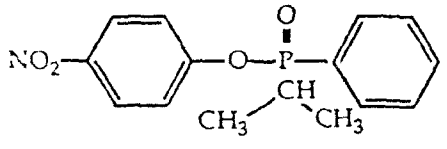

4-NPIPP

$$+ \; 19.5\,O_2 \longrightarrow 15\,CO_2 + H_3PO_4 + HNO_3 + 6\,H_2O \qquad (2)$$

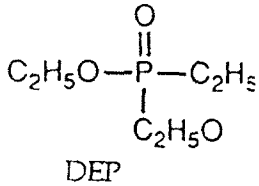

DEP

$$+ \; 9.5\,O_2 \longrightarrow 6\,CO_2 + H_3PO_4 + 6\,H_2O \qquad (3)$$

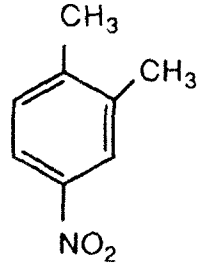

NOX

$$+ \; 10.5\,O_2 \longrightarrow 8\,CO_2 + 4\,H_2O + HNO_3 \qquad (4)$$

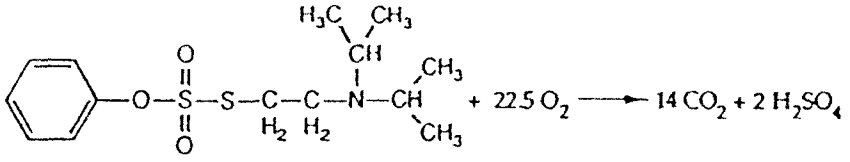

TSPAP

$$+ 22.5\,O_2 \longrightarrow 14\,CO_2 + 2\,H_2SO_4 + HNO_3 + 9\,H_2O \quad (5)$$

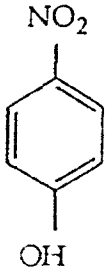

4-NP

$$+ 7\,O_2 \longrightarrow 6\,CO_2 + HNO_3 + 2\,H_2O \quad (6)$$

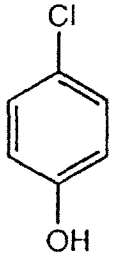

4CP

$$+ 6.5\,O_2 \longrightarrow 6\,CO_2 + HCl + 2\,H_2O \quad (7)$$

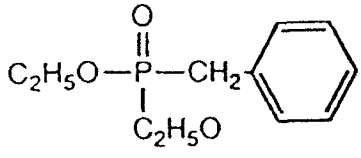

DBP

$$+ 15\,O_2 \longrightarrow 11\,CO_2 + H_3PO_4 + 37\,H_2O \quad (8)$$

Fe(III) ions catalyze efficiently the total oxidation of simulants by H_2O_2

The usage of Fe(III) salts such as $Fe_2(SO_4)_3$, $Fe(NO_3)_3$ and $FeCl_3$ as a catalyst in these degradation reactions proved to be an important discovery. $Fe_2(SO_4)_3$ and $Fe(NO_3)_3$ are cheap and readily available compounds which have no harmful effect on the environment. They were found to greatly accelerate the total oxidation of phosphate ester simulants in aqueous environment even at relatively low concentrations.

The catalytic effect of $Fe_2(SO_4)_3$ is demonstrated in Fig. 1 where the thermal decomposition of 4-NPIPP (4-nitrophenylisopropylphenyl phosphinate) evaluated by CO_2 evolution as a function of catalyst concentration is depicted.

All aqueous dispersions were prepared by the following technique. The appropriate quantity of 10^{-1} M simulant solution (THF solvent) was injected onto the reaction vessels' walls and the solvent evaporated until no traces of solvent were left. Subsequently, the simulant was redissolved in water, and the appropriate catalytic agents [here, $Fe_2(SO_4)_3$] added, the solutions being stirred continuously. This reaction was followed by analysis of the CO_2 evolved. High pressure liquid chromatography (HPLC) data confirmed quantitatively these decomposition reactions through reactant loss.

Fig. 1 shows that the degradation of 4-NPIPP ($7 \cdot 10^{-4}$ M) at 50°C goes progressively faster and nearer to completion as the concentration of $Fe_2(SO_4)_3$ increases (only a small difference in reaction rate and yield is noted between the two upper concentration limits of $5 \cdot 10^{-3}$ M and $1 \cdot 10^{-2}$ M). At these Fe(III) concentrations the mineralization of the simulant is achieved within minutes while in the absence of Fe(III) only a small fraction of the agent was degraded after 2.5 hours.

In order to rationalize this dramatic catalytic effect we evoke tentatively the participation of iron species having a higher oxidation state than III. Since Fe(II) displays significantly lower catalytic activity in the decomposition of phosphate esters than Fe(III) a simple Haber-Weiss type mechanism alone cannot explain the present observations. At pH's greater than 2 (this experimental work is generally carried out at pH's between 5 and 6) iron (III) is highly hydrolyzed and forms oligomeric structures:

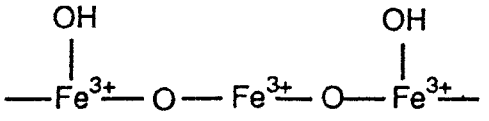

The rapid oxidation of the organophosphate compounds takes place by reaction with an Fe(IV) complex, an extremely powerful oxidant, formed by O-transfer from hydrogen peroxide, according to the following reaction:

$$\left[-\overset{\overset{OH}{|}}{Fe}-O-\right]_n + H_2O_2 \longrightarrow H_2O + OH^- + \left[-\overset{\overset{O}{\|}}{Fe}(IV)^+-O-\right]_n$$

As the organophosphate is subsequently oxidized Fe(IV) is regenerated into Fe(III), thus maintaining its catalytic status. Hydrogen peroxide is exhausted as a sacrificial oxidant.

Amongst these various ferric salts examined, $Fe(NO_3)_3$ appeared to be the most catalytically active, the initial reaction rate being very rapid attaining the theoretical total decomposition threshold within 30 minutes. The age of the catalytic preparation apparently has an effect on its catalytic activity, freshly prepared catalysts being much more active. This decline in activity upon ageing is most likely due to iron hydroxide formation, a form proven experimentally to be inactive catalytically in promoting these decompositions. Iron to toxic compound ratios greater than 1 to 1, i.e., either 3 to 1 or 2 to 1 likewise enhance the initial reaction rates.

Titanium dioxide sustains the oxidizing action of hydrogen peroxide by formation of surface peroxides

TiO_2 plays a stabilizing role in these experiments. This effect is shown in **Fig. 2** at 70°C and at constant concentration of $Fe_2(SO_4)_3$ (i.e., 10^{-3} M) where the decomposition of 4-NPIPP (CO_2 evolution) at various concentrations of H_2O_2 is illustrated. Without TiO_2 present the lower concentrations of H_2O_2 are much less effective in the decomposition of 4-NPIPP than when TiO_2 is present at 5 gm/l. In TiO_2 containing solutions there is very little difference in degradation efficiency between 0.02 M and 1 M H_2O_2. The surface of TiO_2 must therefore play a decisive role in sustaining the oxidative action of H_2O_2. In TiO_2-free solution the H_2O_2 decomposes by disproportionation into oxygen and water. This competes with the H_2O_2 reaction with agent explaining the incomplete nature of simulant degradation at the lower H_2O_2 concentration. In the presence of TiO_2 the H_2O_2 is bound to the surface forming titanium peroxo complexes which do not undergo such disproportionation. The important role of TiO_2 which emerges from these

studies is that it stabilizes the peroxide while maintaining its high oxidation power.

Photocatalytic decomposition

The oxidative destruction of the organophosphate was also examined in solutions containing (apart from the hydrogen peroxide) only ferric sulfate. This led to the surprising and important discovery that simulated sunlight enhances this process even in the absence of titanium dioxide.

Further investigations were carried out in order to explore whether or not ferric sulfate was also effective in catalysing the complete decomposition of the organophosphate in the absence of light. This effect is indeed confirmed by the results shown in **Fig. 3** for DBP. The decomposition was studied here in the dark at 50°C and at room temperature. In the presence of ferric sulfate, the CO_2 evolution augments very rapidly even though no light is employed to photo-activate the catalyst. Illumination, however, enhances this effect dramatically. Ferric sulfate, thus, plays a dual role in the mineralization of DBP: it is a potent oxidation catalyst in the dark, and this property is further enhanced by sunlight excitation.

Graphic depiction of the degradation reactions of the simulant species, DEP, NOX, TSPAP, 4-NP and 4-CP in aqueous H_2O_2 solutions containing Fe(III) oligomers are shown in **Figs. 4-8**.

The simulants DBP and KHP were used as model compounds in order to elucidate the mechanism in the Fe(III) catalyzed H_2O_2 oxidant photodegradations where peroxidase-type activity is presumed to prevail.

Fig. 9 shows the decline of the percentage of TOC present in the solution as well as the increase in the amount of CO_2 generated as a function of reaction time. The solutions contained 10^{-2} M $Fe(NO_3)_3$ and 0.3 M H_2O_2 in addition to $5x10^{-3}$ M DBP. In the beginning the pH of the DBP solution was 5.9, decreasing to 2.25 after $Fe(NO_3)_3$ addition. H_2O_2 addition initially caused a further decrease of the pH to 1.6 followed by an increase in the pH to a value of 1.75 after complete mineralization of the DBP. The CO_2 is expressed in units of percentage conversion with respect to the stoichiometry of **eq. 8**, which describes complete mineralization of the organo-phosphonate.

In the presence of DBP, H_2O_2, and $Fe(NO_3)_3$, a long-lived Fe-oxo-DBP complex is formed which can be light-activated even after 8 days of standing to produce the presumed high-valent iron-oxo complex. This peroxidase-type complex initiates oxidation of its ligand, DBP, with rapid CO_2 formation. The decline in activity several days after preparation is probably due to competitive

Fe-oligomer formation rendering a decreased production of the active intermediate high-valent mononuclear Fe-oxo species.

Direct evidence for the formation of this intermediate was obtained by optical absorption spectroscopy (**Fig. 10**). Upon addition of H_2O_2 to solutions containing DBP and $Fe(NO_3)_3$, the solution turns intensely black-brown. The color fades rapidly within a few minutes to yield a brownish-yellow-colored species. The difference spectrum obtained 2 minutes after mixing [ref. solution DBP and $Fe(NO_3)_3$] has a maximum at 380 nm and a tail extending through the entire visible region until 800 nm with a shoulder around 550 nm. The long wavelength tail of this spectrum decays within only a few minutes, while at shorter wavelengths the decrease is greatly diminished. In the dark at 50°C, about half of the 380 nm absorbance decays within 30 to 60 minutes, the other half being long-lived. Under visible ($\lambda > 435$ nm) light illumination, the 380 nm absorbance disappears very rapidly and completely within less than 10 minutes.

The yellow-brown colored intermediate with λ_{max} at 380 nm is tentatively identified as a high-valency iron complex with DBP. The high potential of Fe in such a complex induces its autodestruction via oxidation of the ligand to CO_2 and release of inorganic phosphate. For reasons which need to be explored, this reaction is biphasic in the dark, the faster and slower part contributing about equally to the decomposition. The intermediate Fe species' oxidizing power is strongly enhanced by visible light.

The mode of addition of H_2O_2 on the degradation reaction of DBP influences the completion of the reactions. Thus, three subsequent additions of 0.6 equivalents of H_2O_2 result in the same ultimate yield of CO_2 as two equivalents added initially. The catalytic destruction of H_2O_2 by $Fe(NO_3)_3$ is at least partially circumvented. The ratio of DBP : $Fe(NO_3)_3$ likewise plays a decisive role in the quantitative decomposition of this organophosphonate (**Fig. 11**), the ratio 1:3 exhibiting optimal CO_2 evolution. The nitrate, sulfate, chloride and perchlorate ferric salts were all tested for their efficiency as catalysts, $Fe(NO_3)_3$ being the most effective (**Fig. 12**).

Comparative studies with other catalysts such as $Cu(NO_3)_2$ or TiO_2 in conjunction with H_2O_2, uphold the exceptional enhancement of both the thermal and light-induced catalytic degradation of the organophosphonate, DBP, by peroxo-iron (III) complexes.

Further experiments, in attempts to elucidate the long-lived active intermediate species, were carried out in $Fe(NO_3)_3$, KHP (potassium hydrogen phthalate) and H_2O_2 solutions. Visible light illumination again sharply accelerates the oxidation of the chelating agent, KHP, as shown in **Fig. 13**. The principal conclusion to be drawn from these observations is that these reactions

cannot proceed by a simple Fenton-type reaction yielding the hydroxyl radical, the hydroxyl radical being neither long-lived enough nor photoexcitable to exhibit the type of behaviour witnessed. The active species is thus speculated to be a high-valent iron complex (the formation of which is autocatalytic as described below), exhibiting photoactivity similar to the horseradish peroxidase intermediate complexes, HP I and HP II. Direct evidence for the formation of the long-lived active intermediate was obtained by optical absorption spectroscopy. Formation of peaks at ca. 400 nm and 600 nm are obtained immediately after mixing $Fe(NO_3)_3$, KHP, and H_2O_2, the decay of the λ = 600 nm peak being more rapid than that at 400 nm. It is apparent from the initial slow growth followed by a rapid acceleration in these peaks' development that **formation of the active species is autocatalytic in nature**. An enormous potential degradative capacity of the organic ligands by this intermediate is thus unleashed, leading to exceedingly rapid CO_2 evolution. The absorbance at 400 nm declines in 40 minutes with simultaneous evolution of CO_2, showing a direct link between this species and the decomposition of KHP (**Fig. 14**).

These spectroscopic findings indicate that there are at least two intermediates involved in the mineralization of the organic species. In the case of the organophosphonates, the organic species complexes Fe(III) via the oxygen of the P=O groups, which are known to be excellent σ donors. Upon addition of H_2O_2, a highly colored peroxo complex is formed. As in the case of the violet H_2O_2 adduct of Fe(III) EDTA, the intense visible transition is probably a HOO^{-} Fe(III) charge transfer band (perhaps the peak at 600 nm). In the next step OH^{-} is lost from the complex resulting in the formation of a ferryl species where the formal oxidation state of iron is five. The yellow-brown colored intermediate with λ_{max} at 380-400 nm is once again presumed to be a high-valency iron complex with the appropriate organic species, i.e., DBP, DEP, DREX, chlorophenol, or KHP. As stated previously (DBP),the high potential of Fe in such a complex induces its autodestruction via oxidation of the ligand to CO_2 with concomitant release of inorganic products. Undoubtedly, the activity of this intermediate Fe species is strongly enhanced by visible light resulting in the greatly accelerated and complete mineralization of the appropriate organic ligands. **Scheme 1** illustrates the described mechanism.

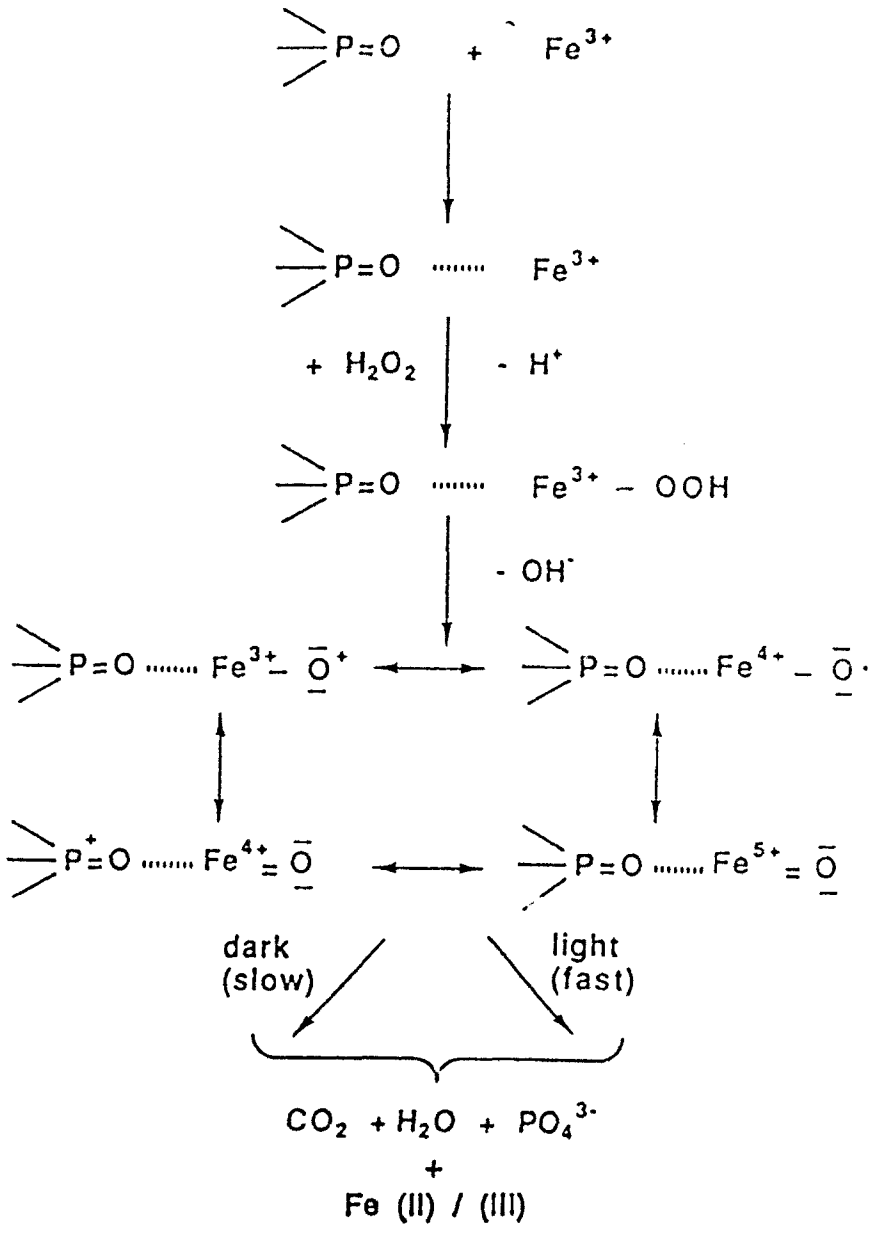

SCHEME 1

Clay supported iron catalysts

Heterogeneous Fe(III) loaded bentonite or montmorillonite clays were also found to exhibit catalytic activity for decomposition of normally difficult to oxidize organic compounds. These compounds form relatively stable complexes with the iron intercalated in the clay layers which can be activated ulteriorly for

decomposition upon the adjunction of H_2O_2, as in the case of the homogeneous iron catalytic solutions.

The pure bentonite clays were prepared according to the following method: 100 gm of pure bentonite (FLUKA), was suspended in 3 l distilled water under stirring for approximately 2 hours. This suspension was then left for 64 hours to decant. The entire solid precipitated and, thus, was resuspended in water and left to stand for approximately 3 hours, where it remained partially in suspension. It was then centrifuged at 4000 rpm for 20 minutes. In order to remove the carbonate, the solid was then suspended in 500 ml 1 M sodium acetate buffer (pH 3.5 acetic acid) and left for ~16 hours. This treatment was followed by repeated washings with water and centrifugation after which it was resuspended in 500 ml 1 M NaCl, centrifuged and resuspended once again in 500 ml 1 M NaCl. The clay was once again washed with water repeatedly and centrifuged until complete removal of Cl^- (as tested by $AgNO_3$).

The iron oxide loaded-bentonite catalysts were prepared according to the following procedure: 250 ml of 0.2 M NaOH were heated to 80°C and added slowly, under vigorous stirring, to 100 ml of 10^{-2} M $FeCl_3$. A brown solution formed. After approximately 20 minutes, the above solution was added slowly to a 0.05% suspension of sodium bentonite in pure water while stirring vigorously. This mixture was stirred for approximately 24 hours and then left to decant for 2 to 3 days. All the clay precipitated. The remaining supernatant contained a considerable quantity of iron. The clay was then centrifuged and washed twice with water, twice with 0.02 N H_2SO_4 or HCl, rewashed with water three times, followed by two final rinsings with absolute ethanol in order to remove excess water. The clay was then dried at room temperature and progressively calcinated at 120°C for 3 hours, at 300°C for 3 hours, and at 500°C for 5 hours. The resulting treated clay contained 1.41 mmoles Fe per gm clay.

In the degradation experiments of 4-nitrophenol and 4-chlorophenol, 120 ml sealed reaction vessels containing 20 ml of either 10^{-2} 4-nitrophenol on 10^{-2}M 4-chlorophenol, 0.6 ml H_2O_2 (~0.23M), and 0.05 gm clay (either pure or iron-loaded) were used. The concentration of DBP (10 ml) used was $5 \cdot 10^{-3}$M with 0.1 gm clay catalyst, whereas the concentration of TSPAP was maintained at $1 \cdot 10^{-3}$M, the clay catalyst concentration being varied. The concentration of H_2O_2 and reaction vessel size remained identical to the experiments using either 4-NP or 4-CP. The CO_2 evolution was followed by testing 500 µl aliquots of the gaseous volume in a GOW MAC gas chromatograph (Parapak column).

Decompositions of the compounds (as evidenced by CO_2 evolution), were tested under several different experimental states in order to ascertain the most efficient conditions. **Fig. 15** compares the differences in the percentages of

photomineralization of aqueous solutions of 4-nitrophenol in presence of Fe-bentonite clay and H_2O_2 at room temperature (28°C) and under heating (60°C). At T = 60°C the 4-nitrophenol is totally decomposed, while at room temperature the decomposition limits itself to approximately 55%. The importance of light for complete mineralization is demonstrated in this figure, where the degradation of 4-nitrophenol (at T = 60°C) in the dark is seen to limit itself to ~64.2%. The synergistic effect of simultaneous irradiation and heating in augmenting the catalytic efficiency of the Fe-bentonite clays is thus demonstrated. The Fe-bentonite clay used in these experiments was washed and rewashed for a second series of experiments (**Fig. 15**). It is shown to maintain its catalytic efficiency even under these recycling conditions as 100% degradation of 4-nitrophenol is again observed. For comparison, the room temperature photodegradation of 4-NP in the presence of pure bentonite clays (**Fig. 16**), results in less than 1% degradation. Dark thermal degradation (T = 60°C) in the presence of pure bentonite clays leads to 59% degradation (**Fig. 16**).

The complementary effect of simultaneous heating and irradiation in presence of Fe-bentonite clays in the decomposition of 4-chlorophenol is demonstrated in **Fig. 17**, where the 4-CP decomposition is seen to be 72.9% in the dark, versus 100% under irradiation at T = 65°C. Room temperature photodegradation of 4-CP in presence of pure bentonite clays leads to only 9% mineralization (**Fig. 18**), whereas that in presence of Fe-bentonite catalyst is much more efficient with 48.6% decomposition. The dark thermal decomposition (T = 65°C) in presence of pure bentonite clay and H_2O is limited to 36.8% (**Fig. 18**).

The total mineralization of the organophosphonate, DBP, in Fe-bentonite suspensions, occurs under simultaneous heating and irradiation, whereas the dark thermal reaction proceeds only until 61.5% (**Fig. 19**). TOC, total organic carbon, measurements corroborate these results.

The thermally assisted (T = 60°C) photodegradation of TSPAP, was tested in the presence of the pure and iron-loaded clay, montmorillonite. TOC measurements exhibited the decomposition of this compound at two different concentrations of the iron oxide-loaded clay as well as in presence of the pure clay (**Fig. 20**).

The degradations in aqueous solutions containing clay-supported Fe(III)-oxide catalytic surfaces and H_2O_2 are seen to proceed as rapidly as those occurring in Fe(III) homogeneous catalytic solutions. The advantage of these clays over homogeneous catalysts lies in their large surface area for reactions and the possibility to recuperate and reutilize the catalyst in ulterior experiments.

CONCLUSIONS

A new, relatively cheap and potent catalyst was discovered in Fe(III) salts, specifically $Fe(NO_3)_3$, where they were shown in our investigations on various pollutant compounds and toxic simulants to be effective both by thermal initiation and under photolysis. The surprising feature of these studies is that the degradative reaction apparently proceeds through a peroxidase-type mechanism (which is enhanced by light) involving a high-valent Fe species, and not through the well-established Haber-Weiss mechanism involving Fe(II)/Fe(III) and hydroxyl radicals which are too short-lived to be the reactive intermediates involved in the experiments discussed herein. These Fe(III) oligomer catalysts can be recycled when supported on bentonite or montmorillonite clays.

THERMAL DEGRADATION OF 4-NPIPP;VARIOUS Fe2 CONCENTRATIONS

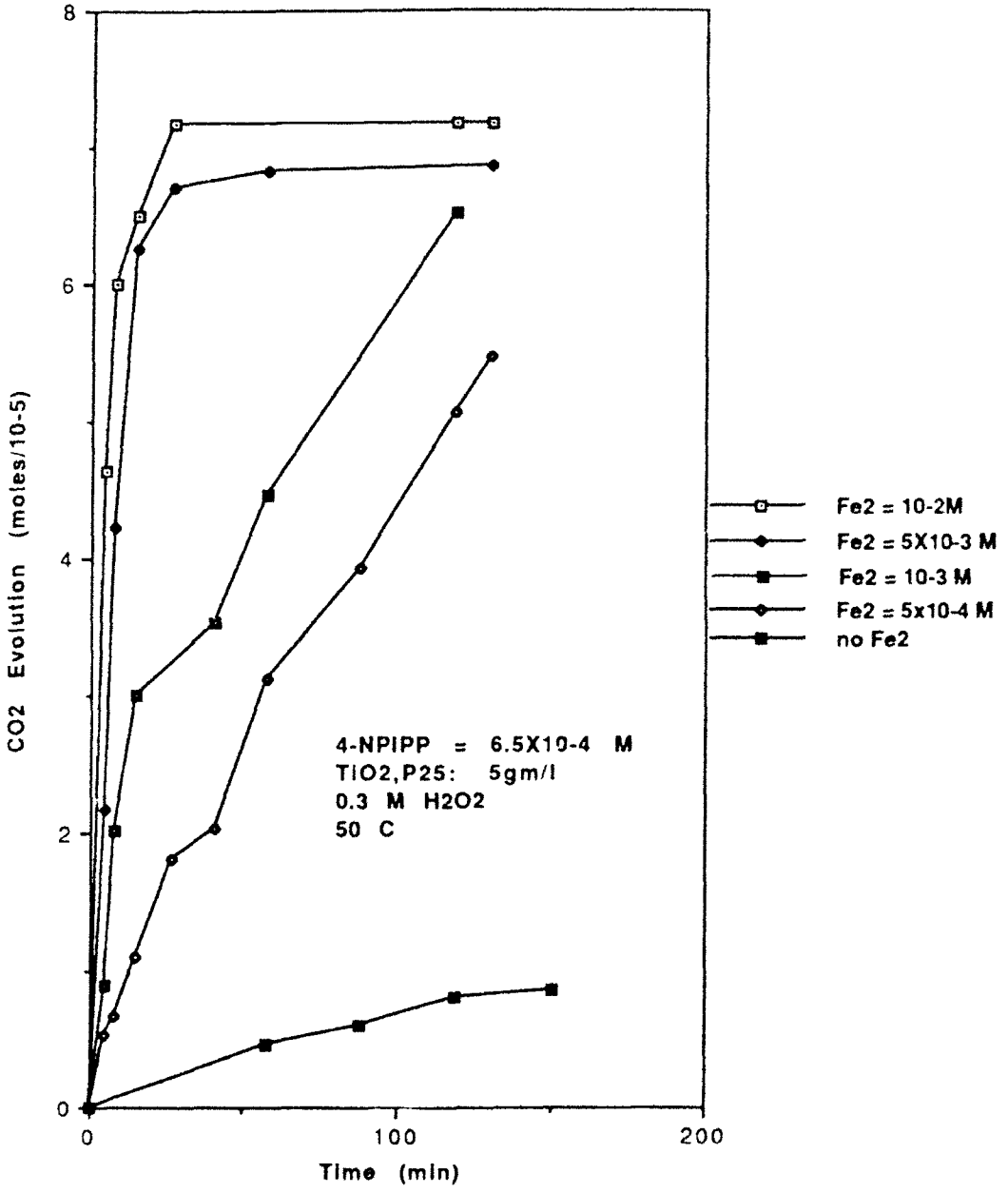

Figure 1

THERMAL DEGRADATION OF 4-NPIPP WITH FE2(SO4)3

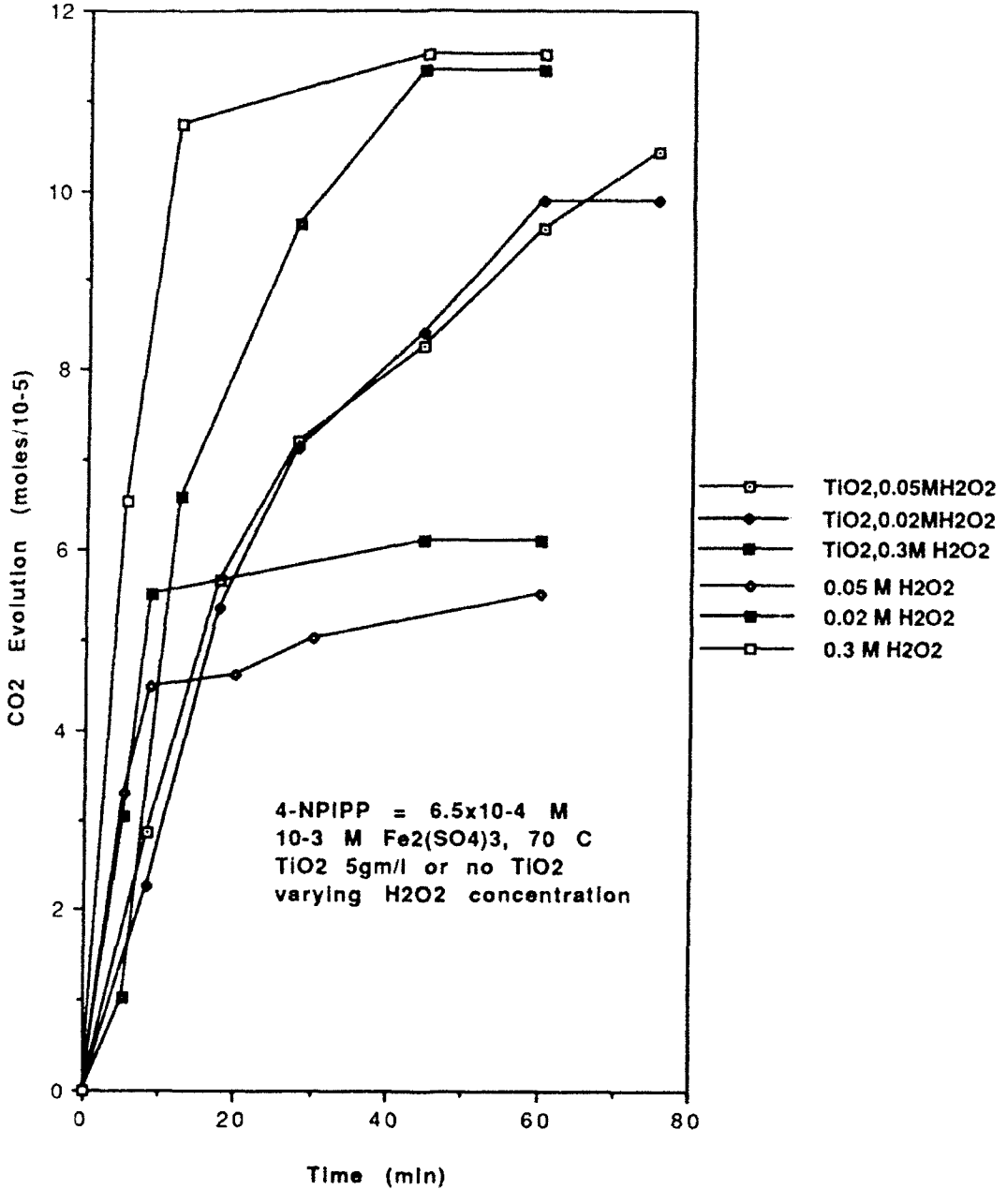

Figure 2

THERMAL & PHOTODEGRADATION OF DBP

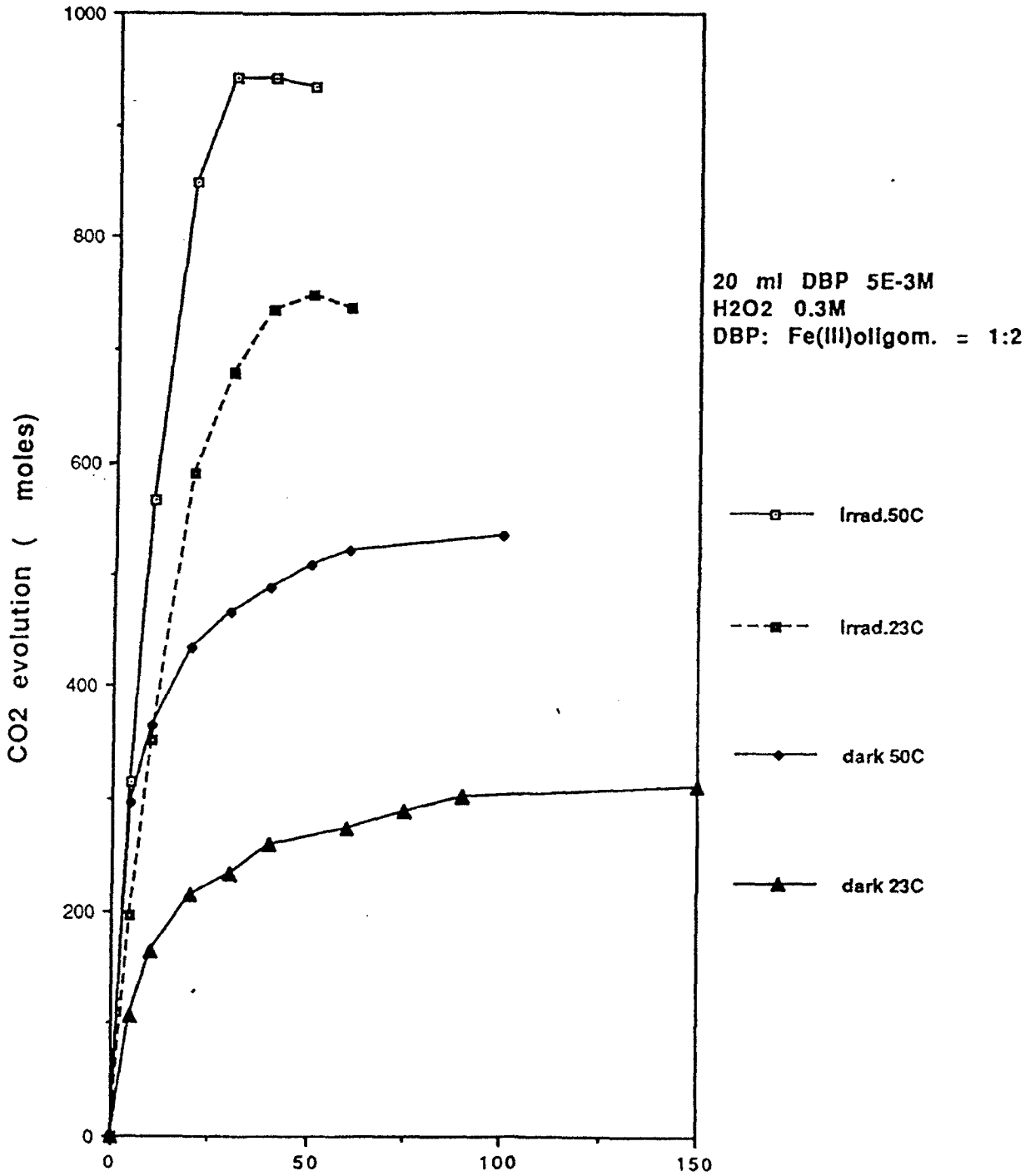

Figure 3

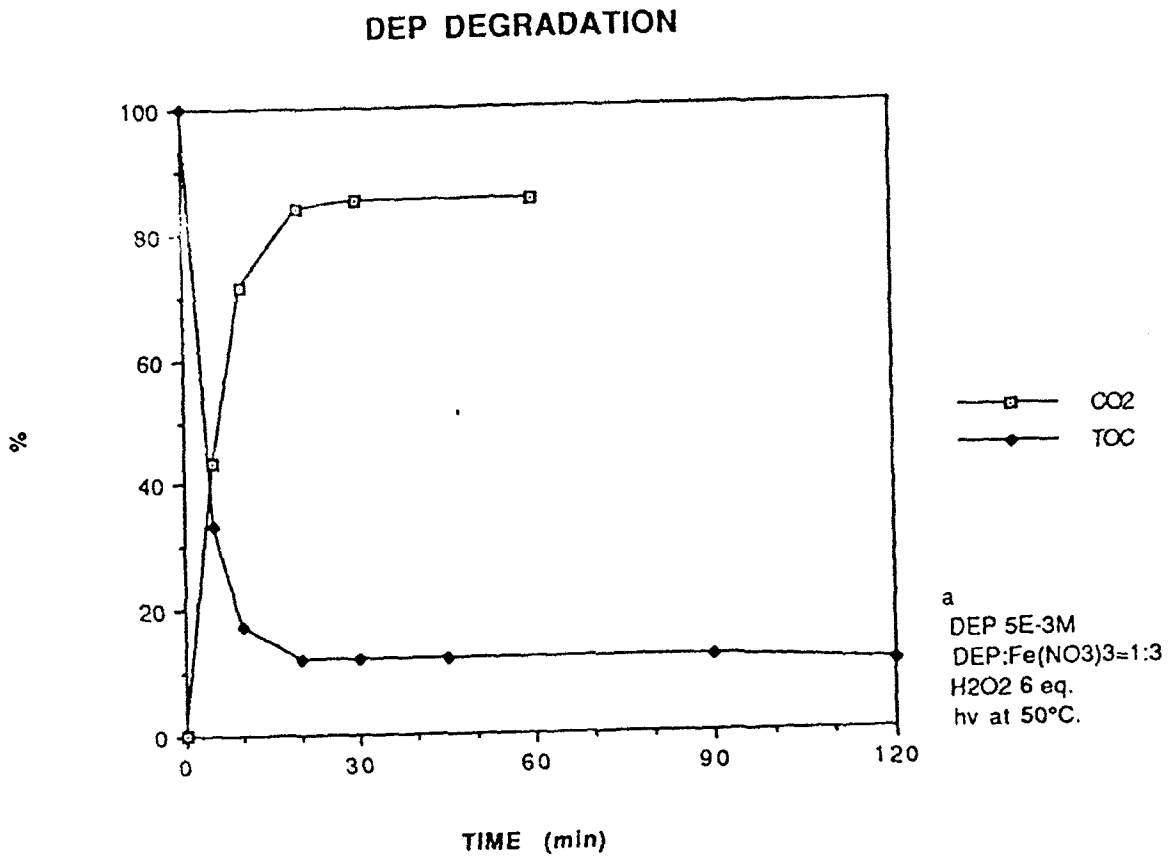
DEP DEGRADATION
100
80
60
40
20
0
%
0
30
60
90
120
TIME (min)
CO2
TOC
a
DEP 5E-3M
DEP:Fe(NO3)3=1:3
H2O2 6 eq.
hv at 50°C.

Figure 4

THERMAL AND PHOTO DEGRADATION OF NITRO-O-XYLENE WITH H2O2 and Fe2(SO4)3 CATALYST

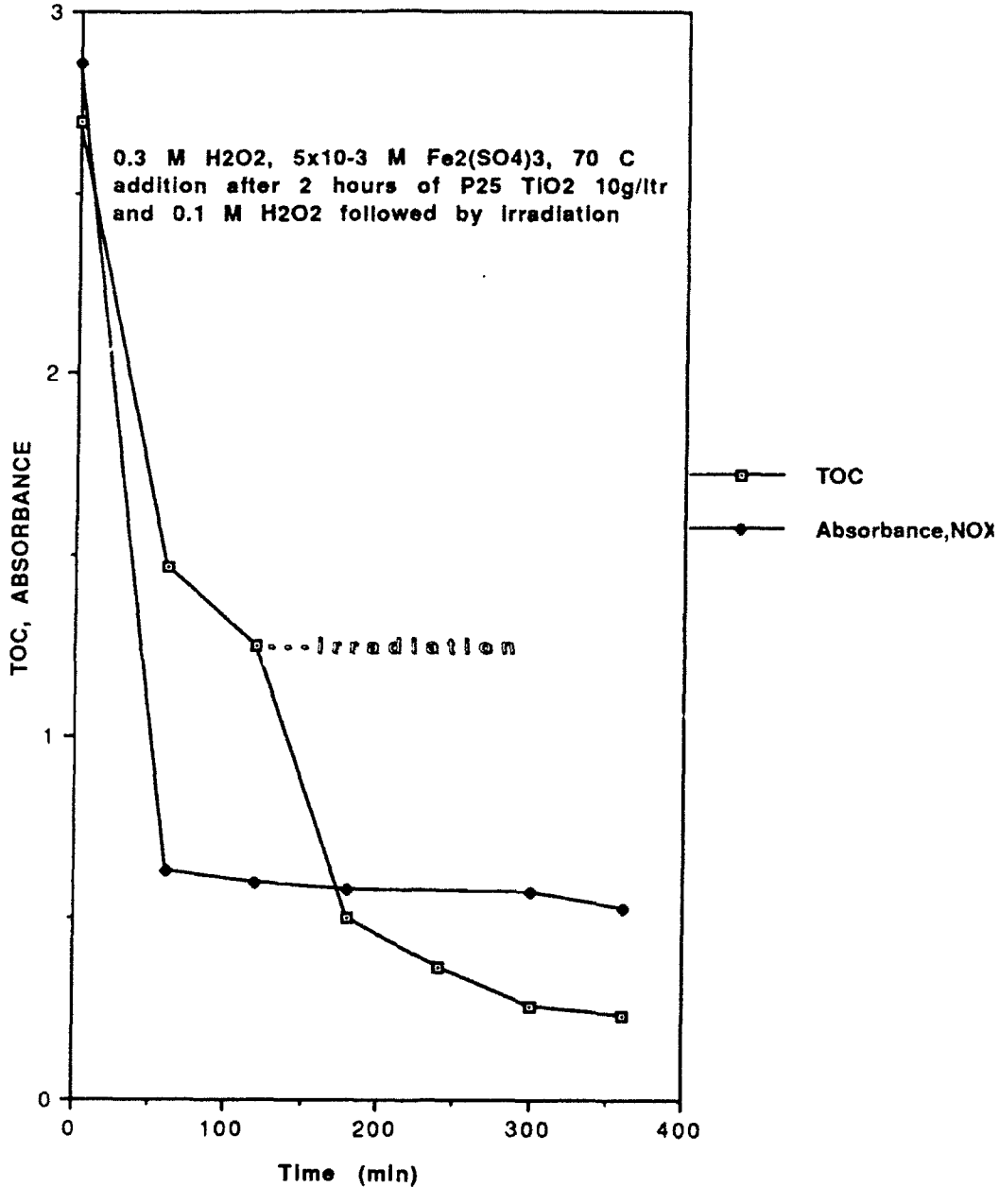

Figure 5

TSPAP photodegradation in presence of FeIII/FeII

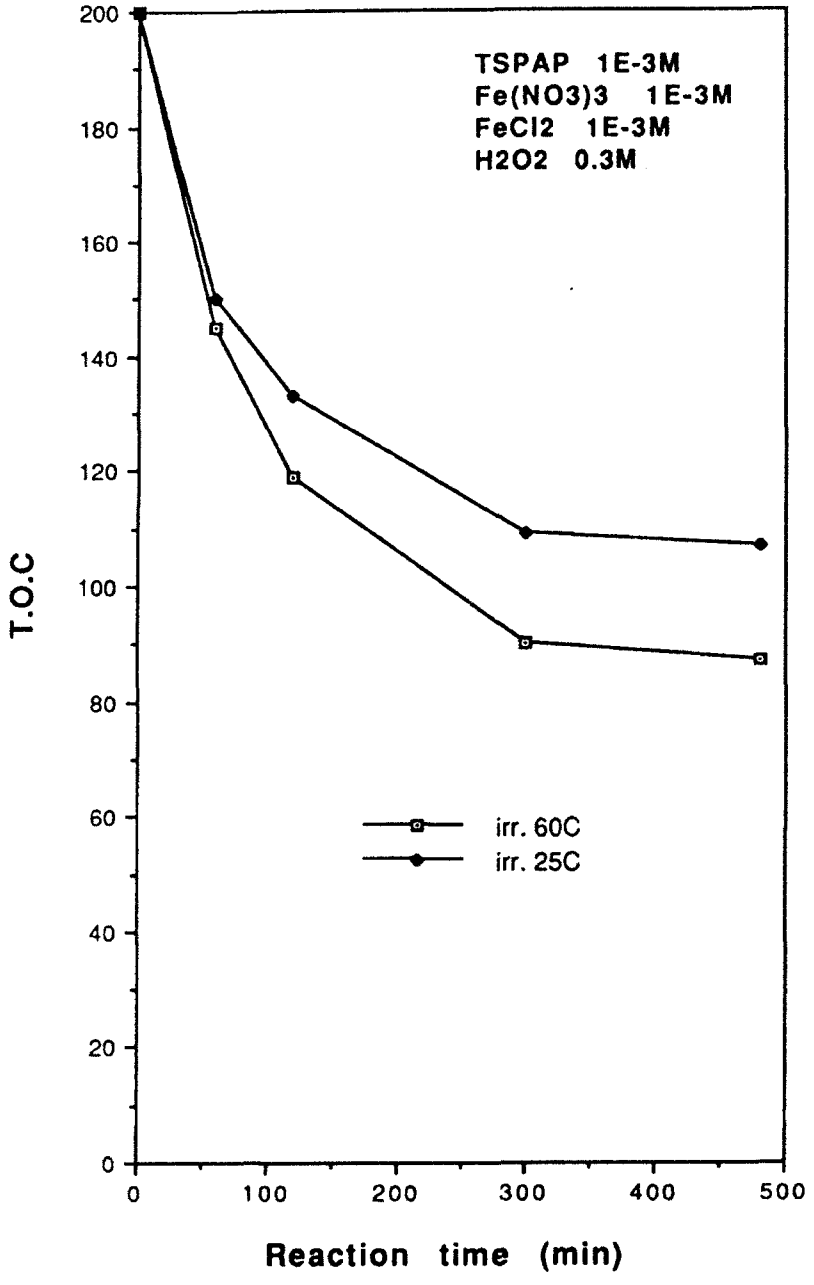

Figure 6

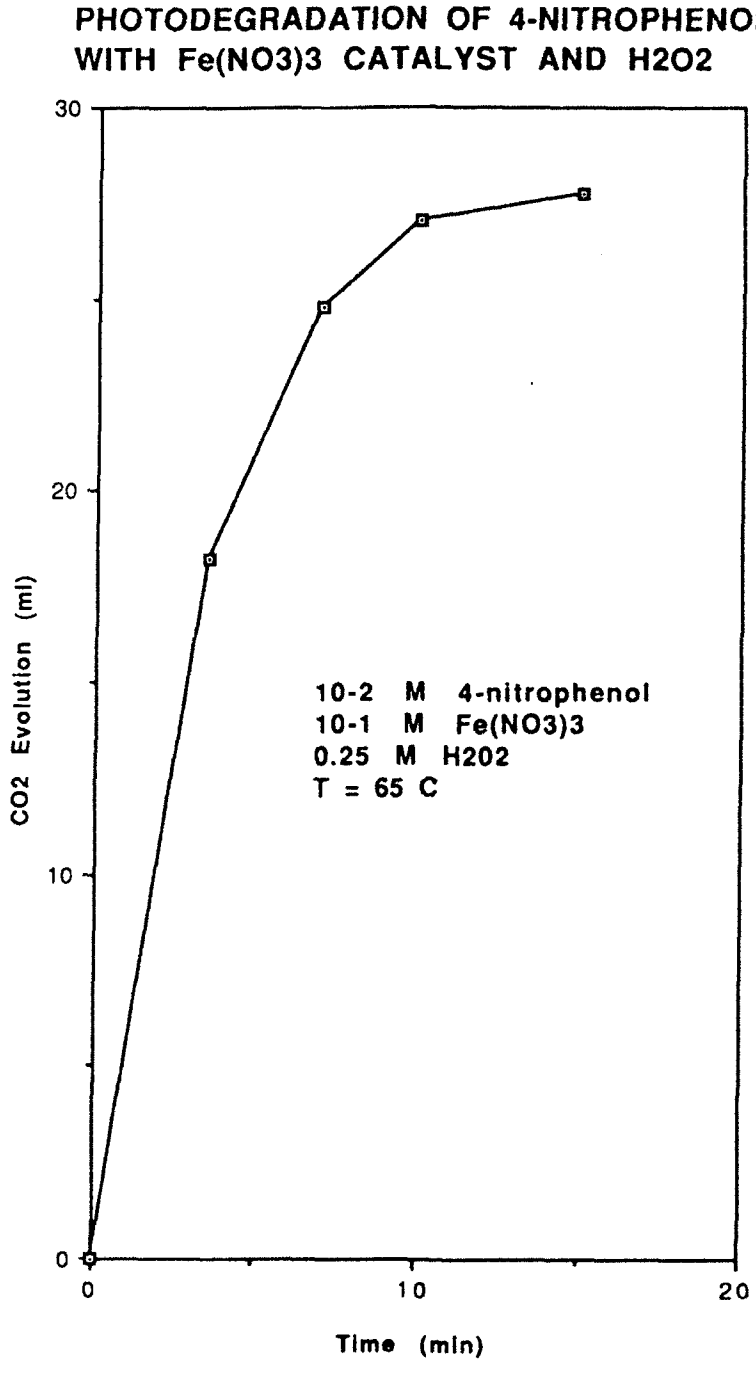
PHOTODEGRADATION OF 4-NITROPHENOL
WITH Fe(NO3)3 CATALYST AND H2O2
30
20
10
0
CO2 Evolution (ml)
10-2 M 4-nitrophenol
10-1 M Fe(NO3)3
0.25 M H202
T = 65 C
0
10
20
Time (min)

Figure 7

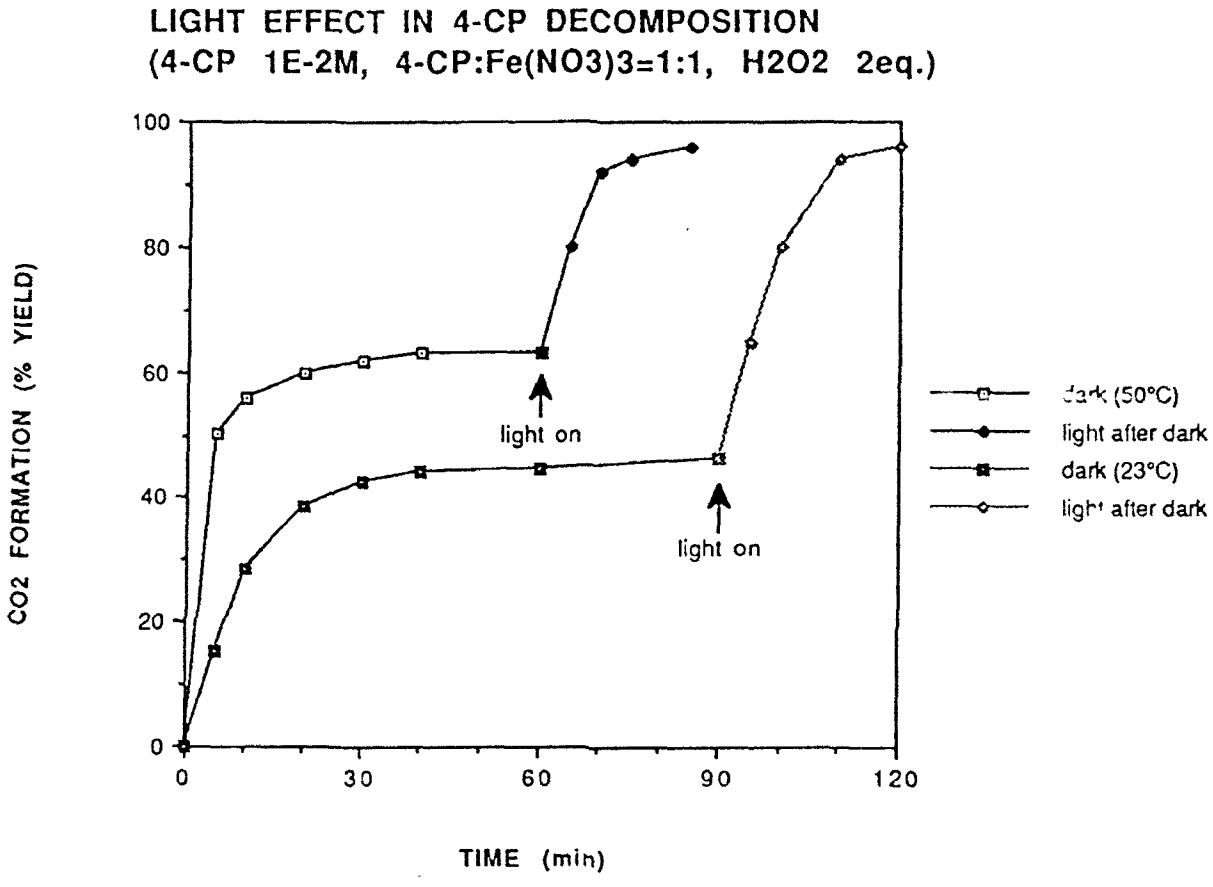
LIGHT EFFECT IN 4-CP DECOMPOSITION
(4-CP 1E-2M, 4-CP:Fe(NO3)3=1:1, H2O2 2eq.)
CO2 FORMATION (% YIELD)
100
80
60
40
20
0
0
30
60
90
120
TIME (min)
light on
light on
dark (50°C)
light after dark
dark (23°C)
light after dark

Figure 8

THERMAL & PHOTODEGRADATION OF DBP

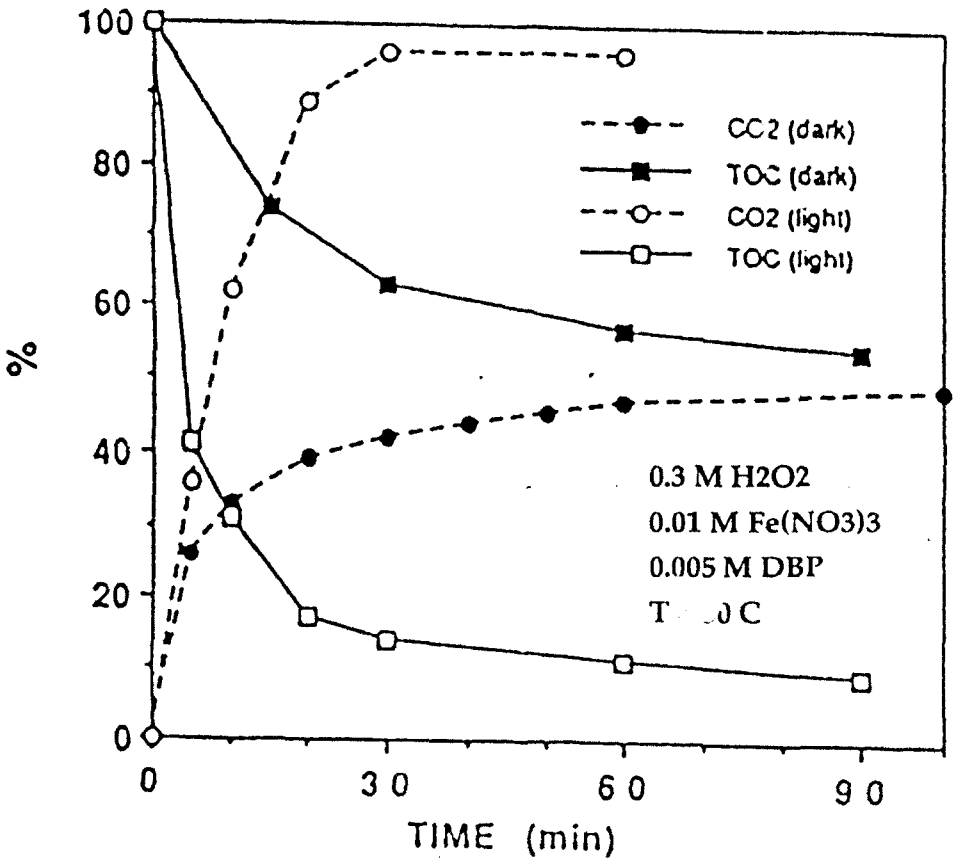

Figure 9

Figure 10

DIFFERENCE SPECTRUM OF DBP, Fe(NO3)3, H2O2 SOLUTIONS

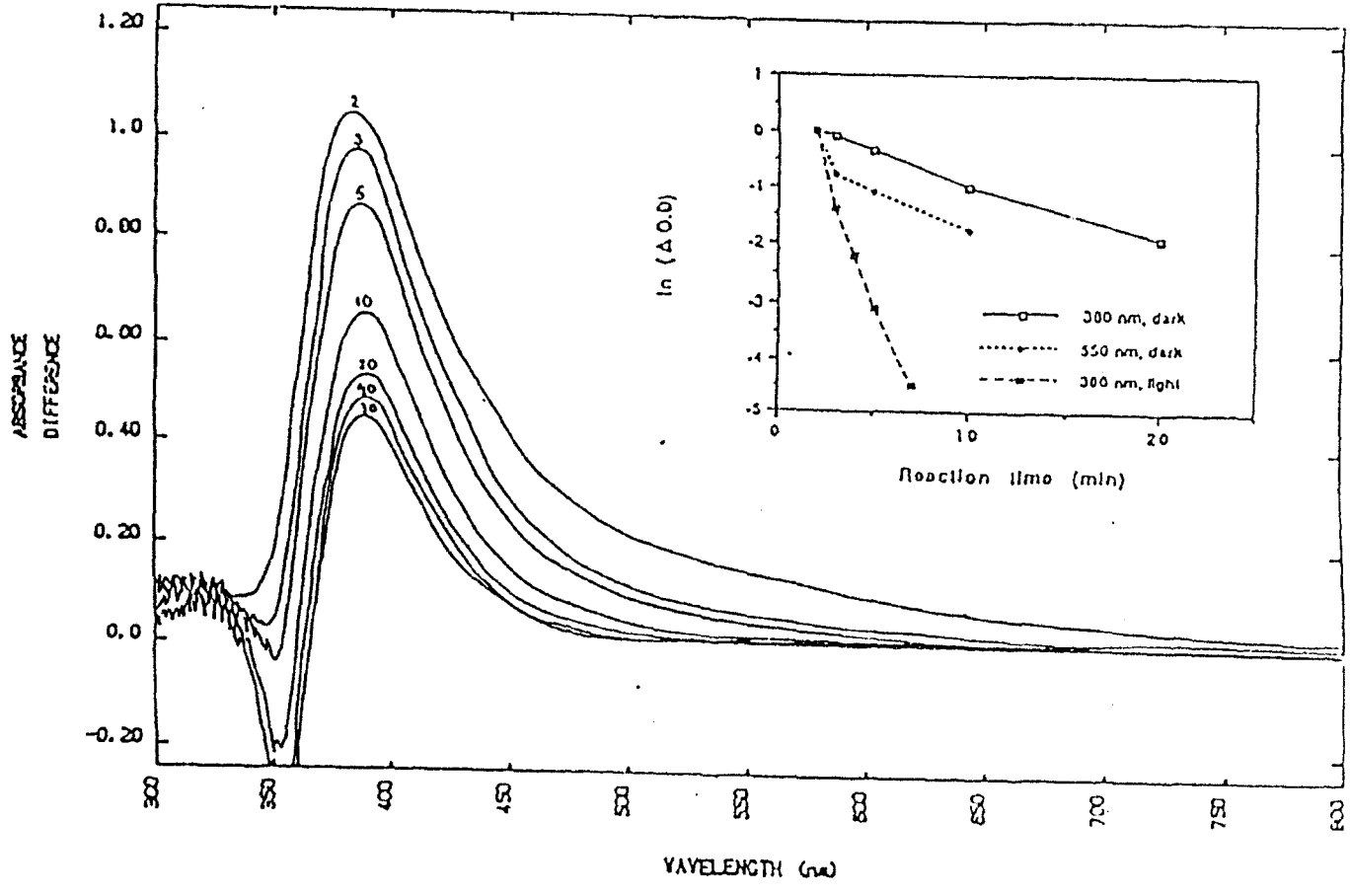

ref. solution: DBP, Fe(NO3)3, no H2O2

inset: absorption decay at 550 and 380 nm after H2O2 addition. Effect of visible light on 380 nm absorption decay

Photodegradation of Diethylbenzylphosphonate (DBP)
by Fe(III) Peroxides
Influence of DBP: $Fe(NO_3)_3$ Ratio

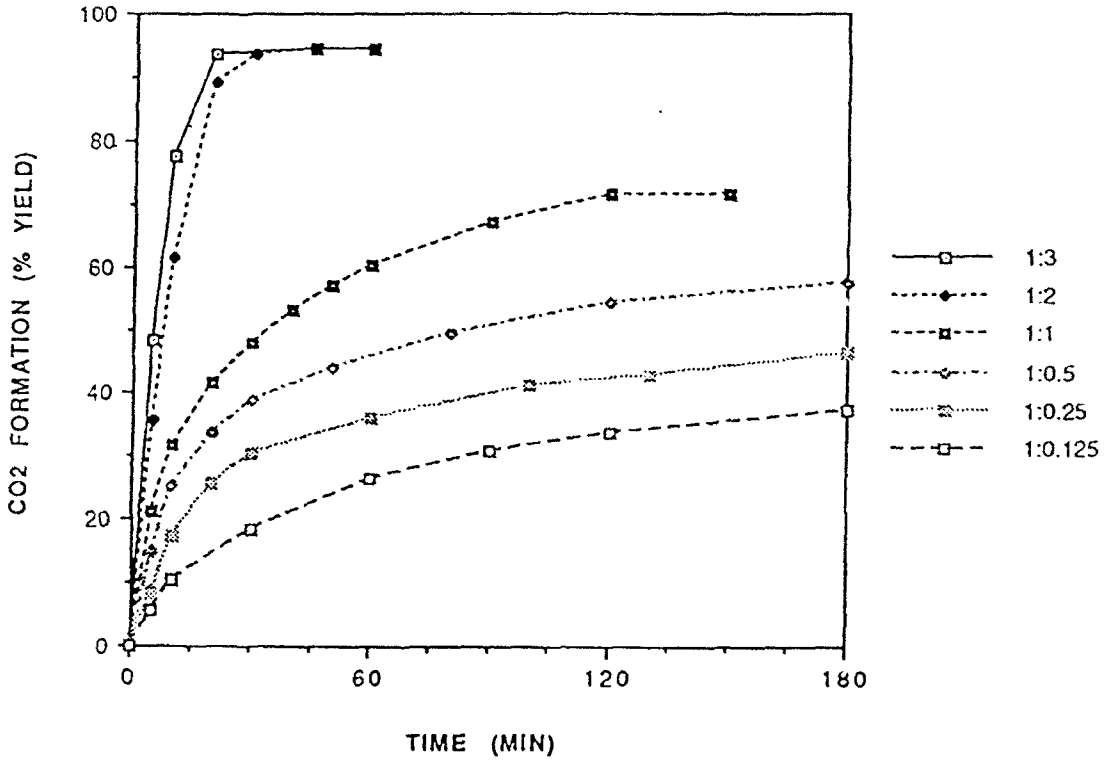

DBP = 5.10^{-3}M, H_2O_2 = 2 equivalents
hv > 435, T = 50°C

Figure 11

Photodecomposition of Diethylbenzylphosphonate (DBP)
in Presence of Various Iron Salts

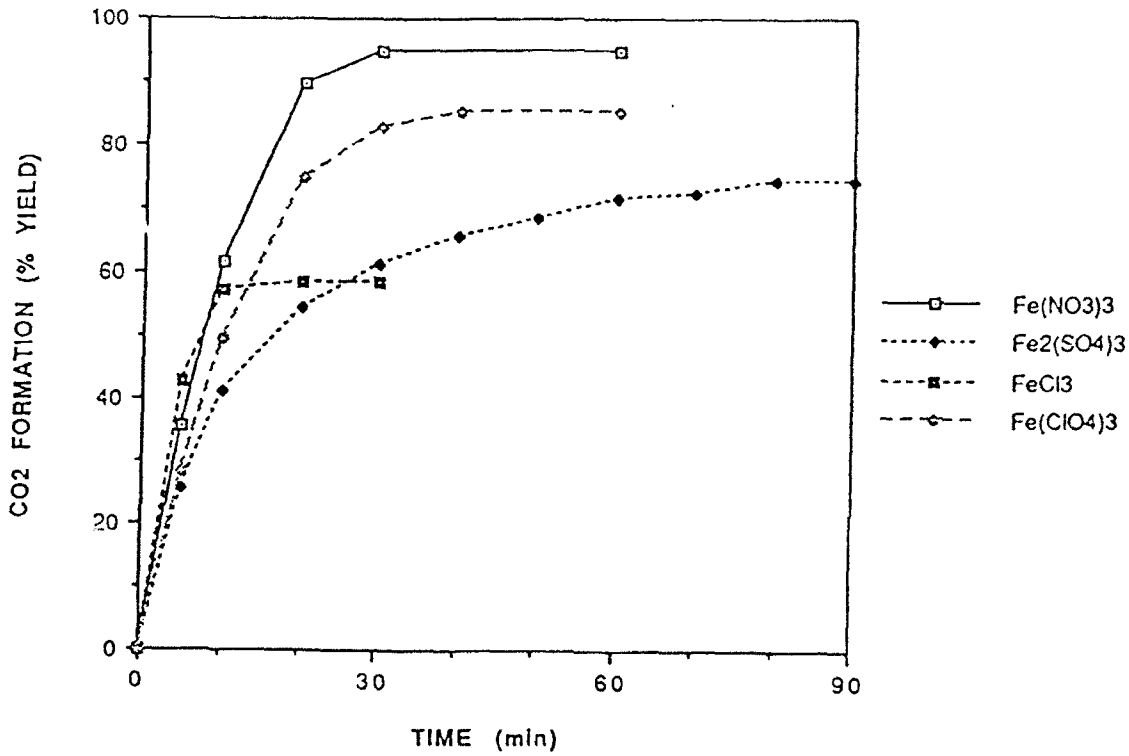

DBP = 5.10^{-3}M, H_2O_2 = 2 eq., DBP : Fe(III) = 1:2,
hv > 435 nm, T = 50°C

Figure 12

CO2 evolution during KHP degradation

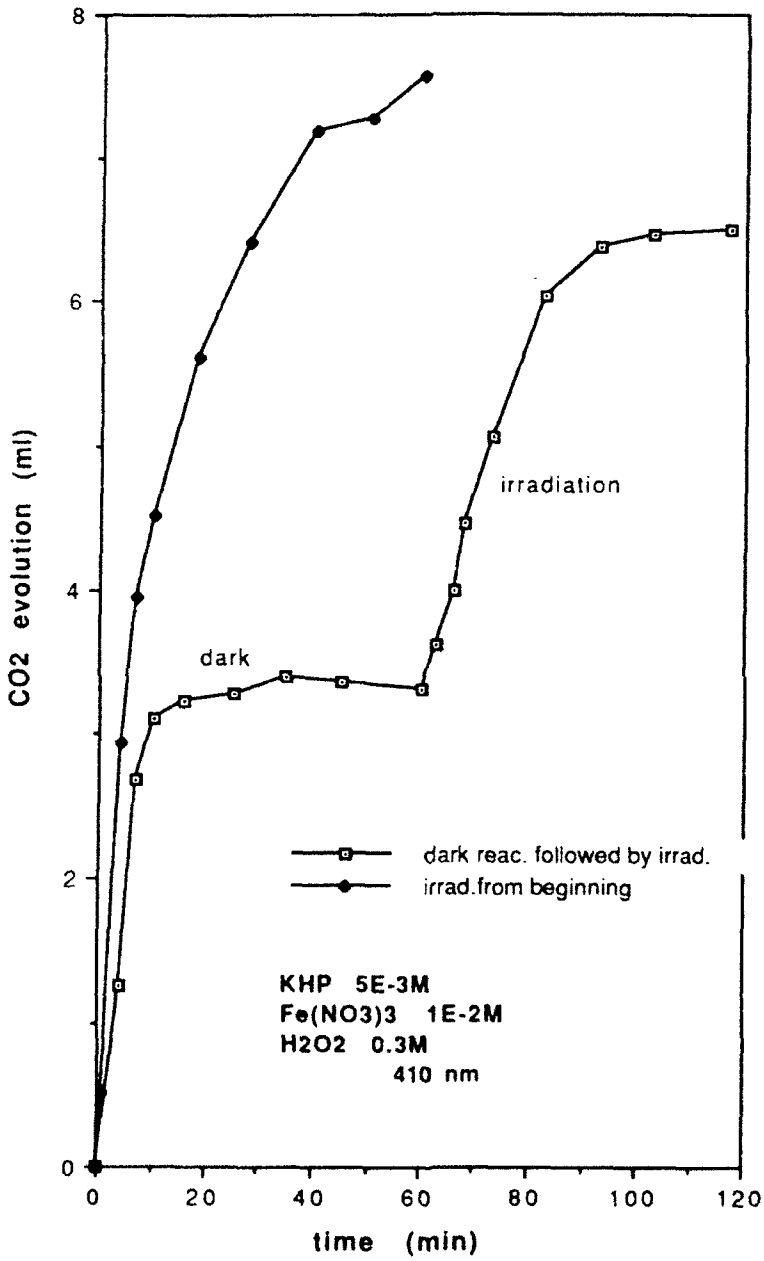

Figure 13

CO2 evolution and 400 nm absorbance decay during KHP degradation

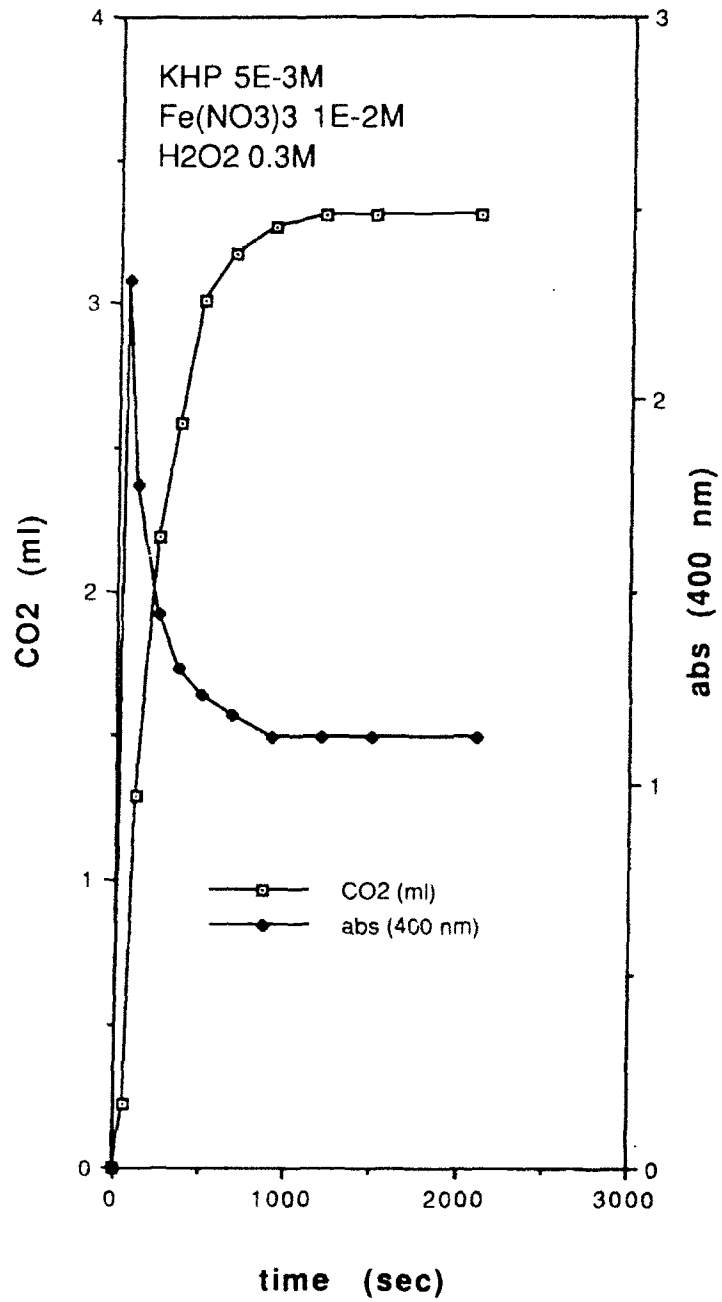

Figure 14

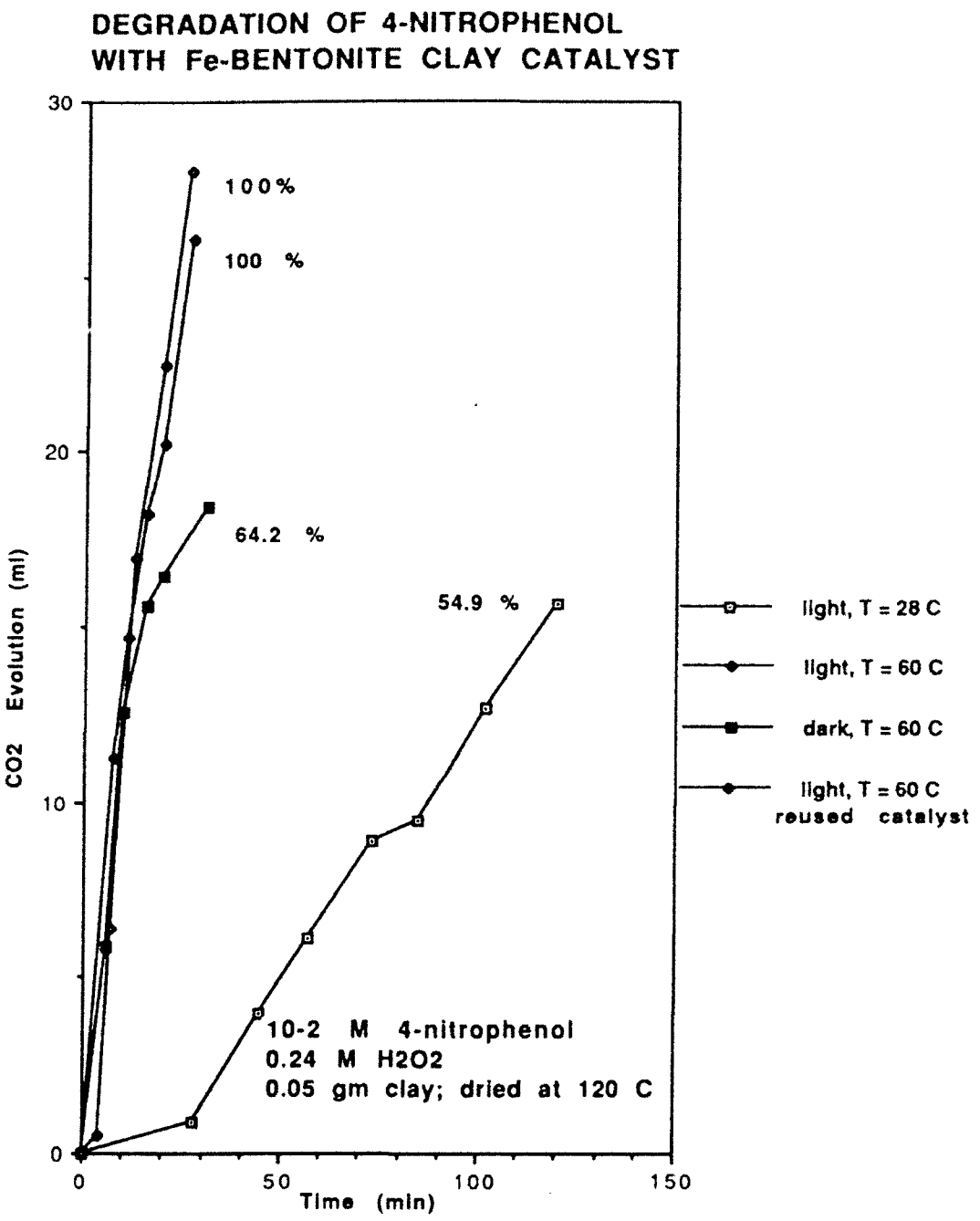
DEGRADATION OF 4-NITROPHENOL
WITH Fe-BENTONITE CLAY CATALYST
30
20
10
0
CO2 Evolution (ml)
0
50
100
150
Time (min)
100%
100 %
64.2 %
54.9 %
10-2 M 4-nitrophenol
0.24 M H2O2
0.05 gm clay; dried at 120 C
light, T = 28 C
light, T = 60 C
dark, T = 60 C
light, T = 60 C
reused catalyst

FIGURE 15

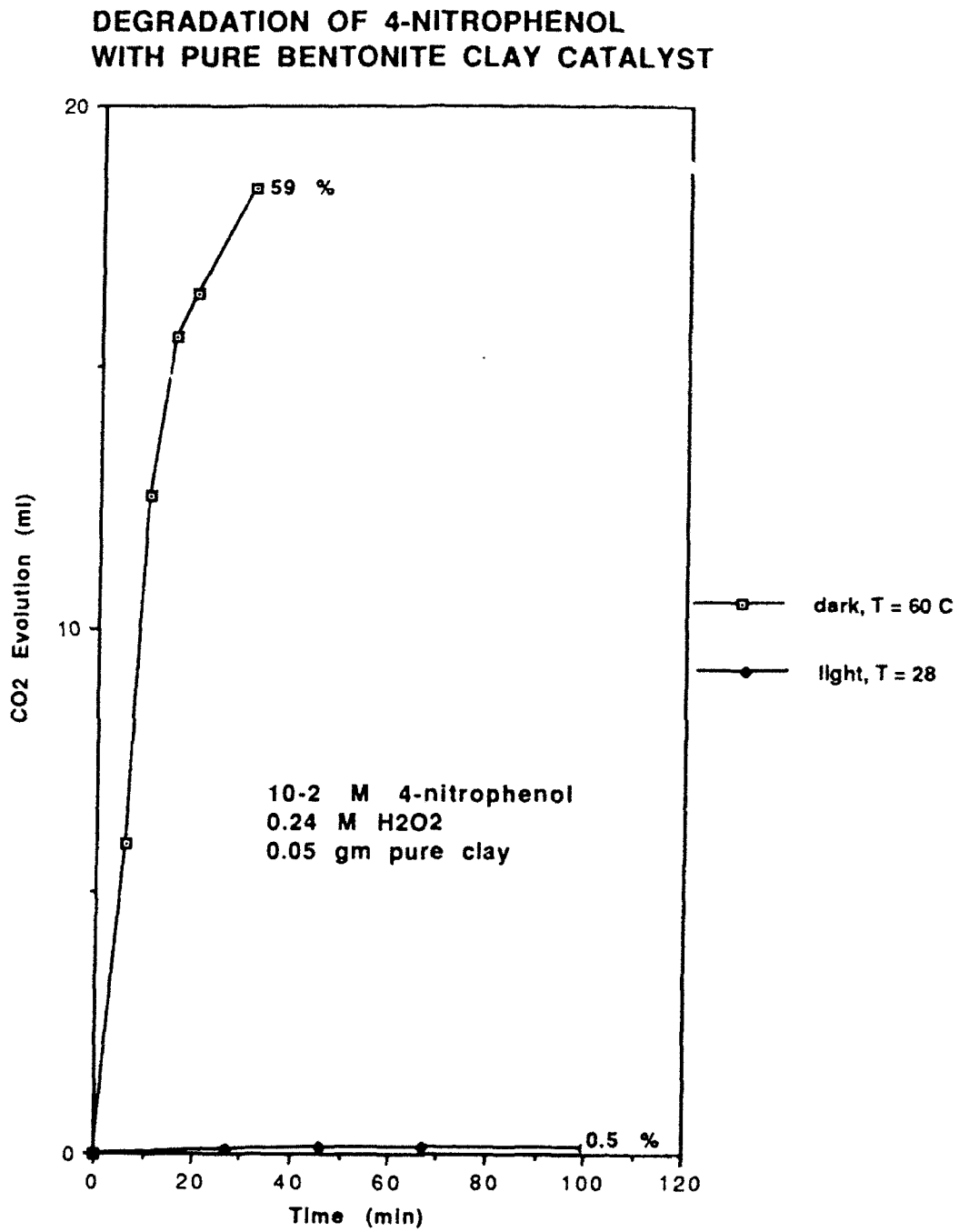
DEGRADATION OF 4-NITROPHENOL
WITH PURE BENTONITE CLAY CATALYST
20
10
0
CO2 Evolution (ml)
59 %
0.5 %
10-2 M 4-nitrophenol
0.24 M H2O2
0.05 gm pure clay
dark, T = 60 C
light, T = 28
0
20
40
60
80
100
120
Time (min)

FIGURE 16

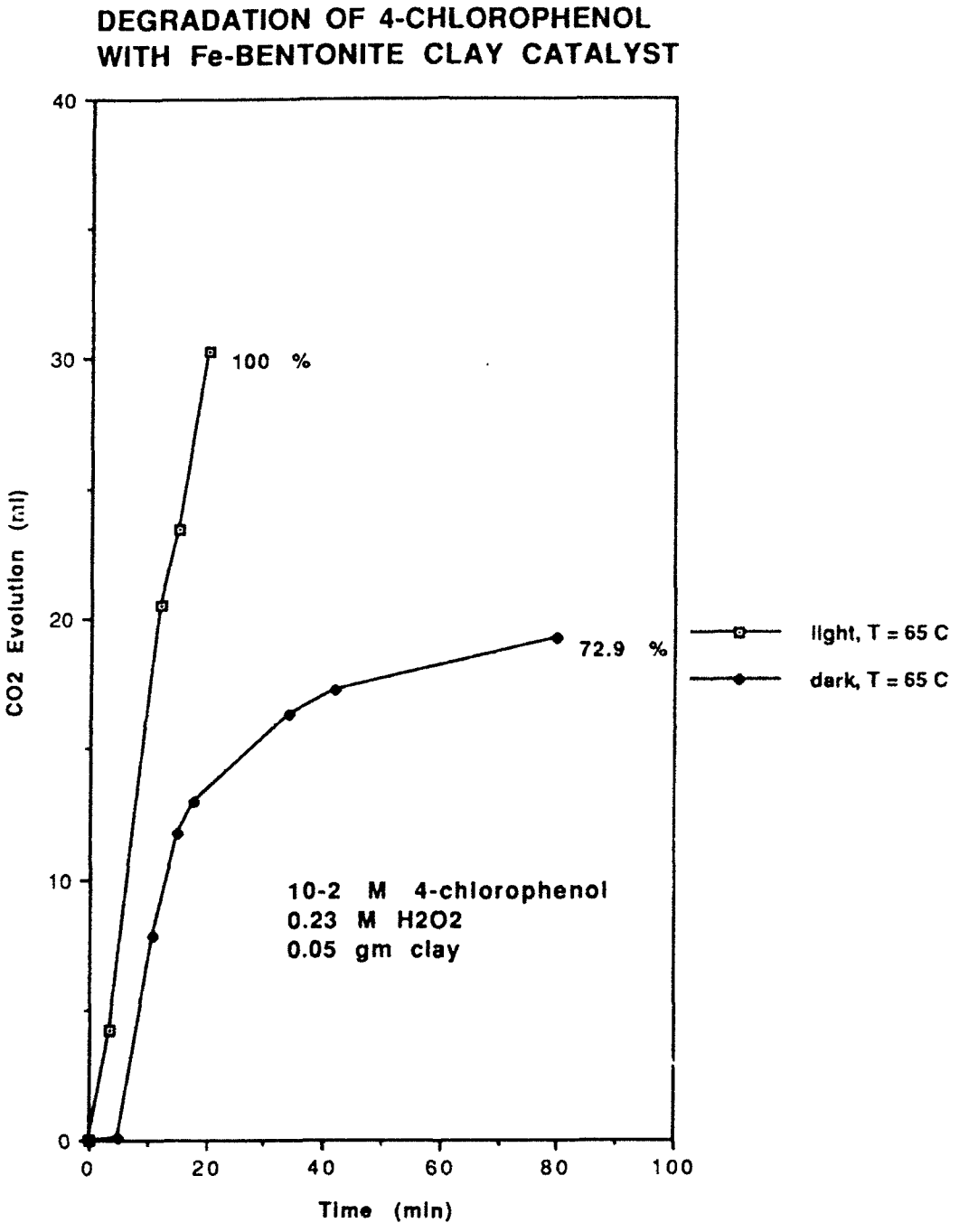
DEGRADATION OF 4-CHLOROPHENOL
WITH Fe-BENTONITE CLAY CATALYST
40
30
20
10
0
CO2 Evolution (ml)
100 %
72.9 %
10-2 M 4-chlorophenol
0.23 M H2O2
0.05 gm clay
light, T = 65 C
dark, T = 65 C
0
20
40
60
80
100
Time (min)

FIGURE 17

DEGRADATION OF 4-CHLOROPHENOL
WITH EITHER Fe-BENTONITE OR
PURE BENTONITE CLAY CATALYSTS

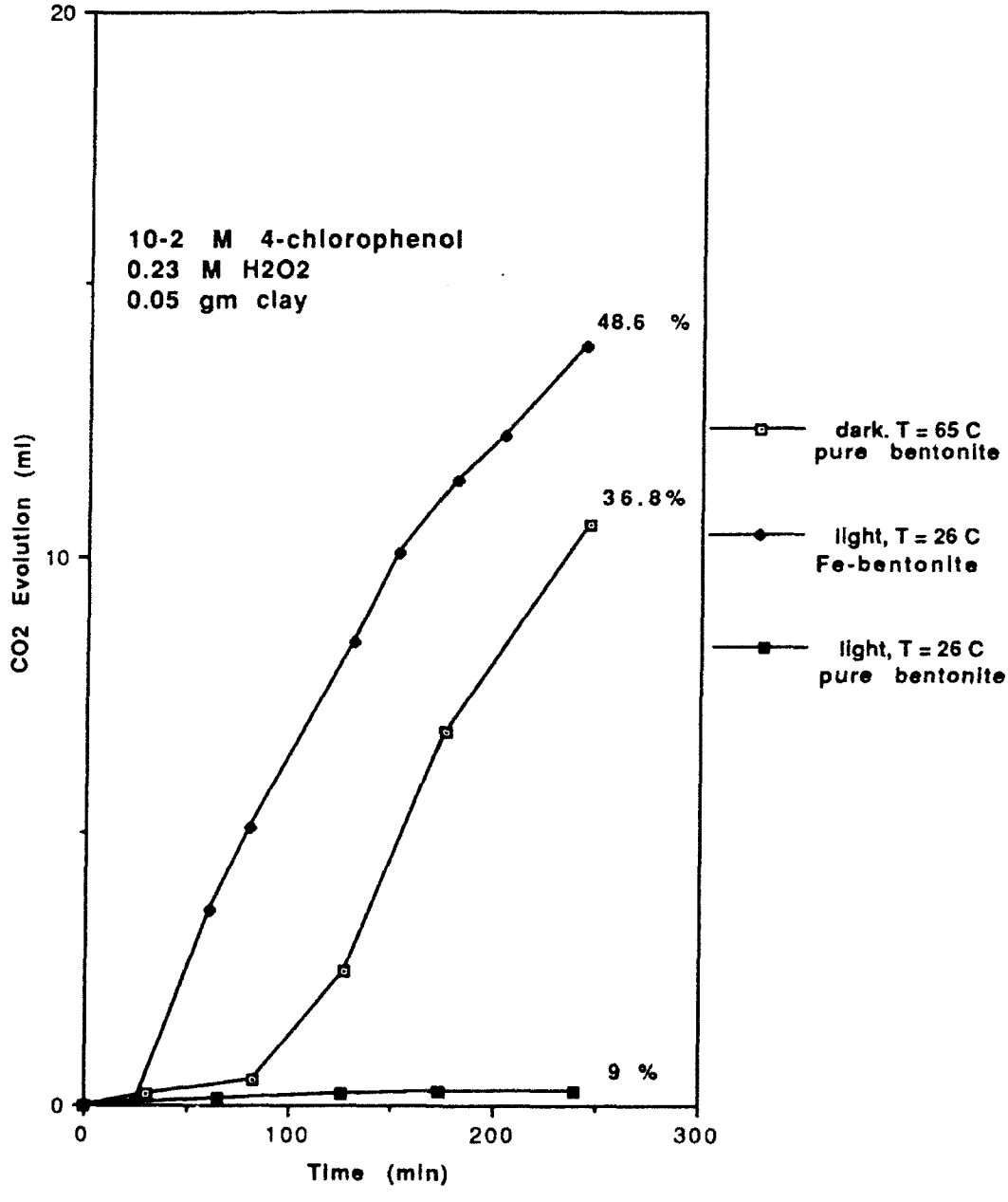

FIGURE 18

DBP Degradation in Fe(III)-Bentonite Suspensions

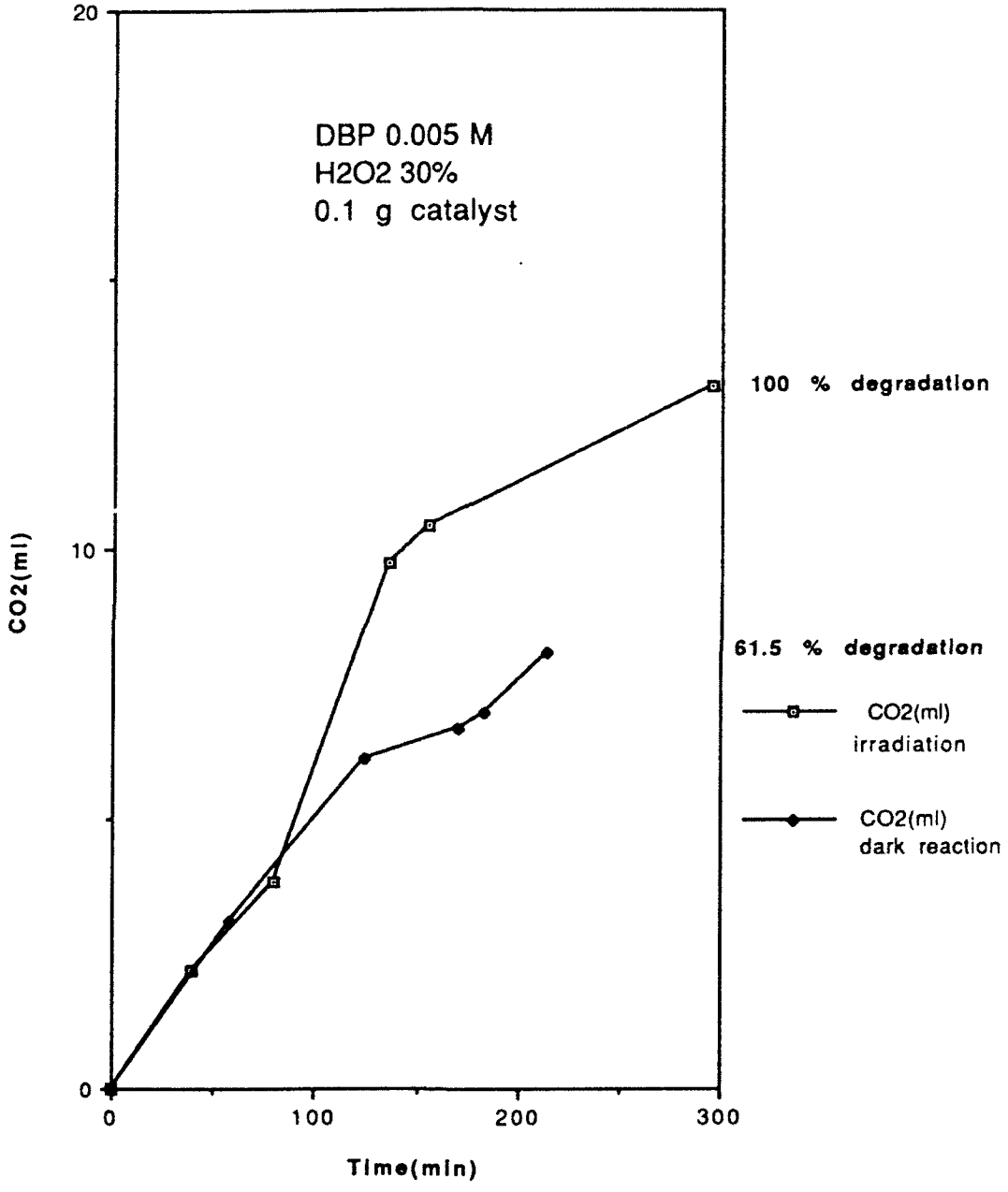

FIGURE 19

TSPAP photodegradation in presence of Fe-montmorillonite

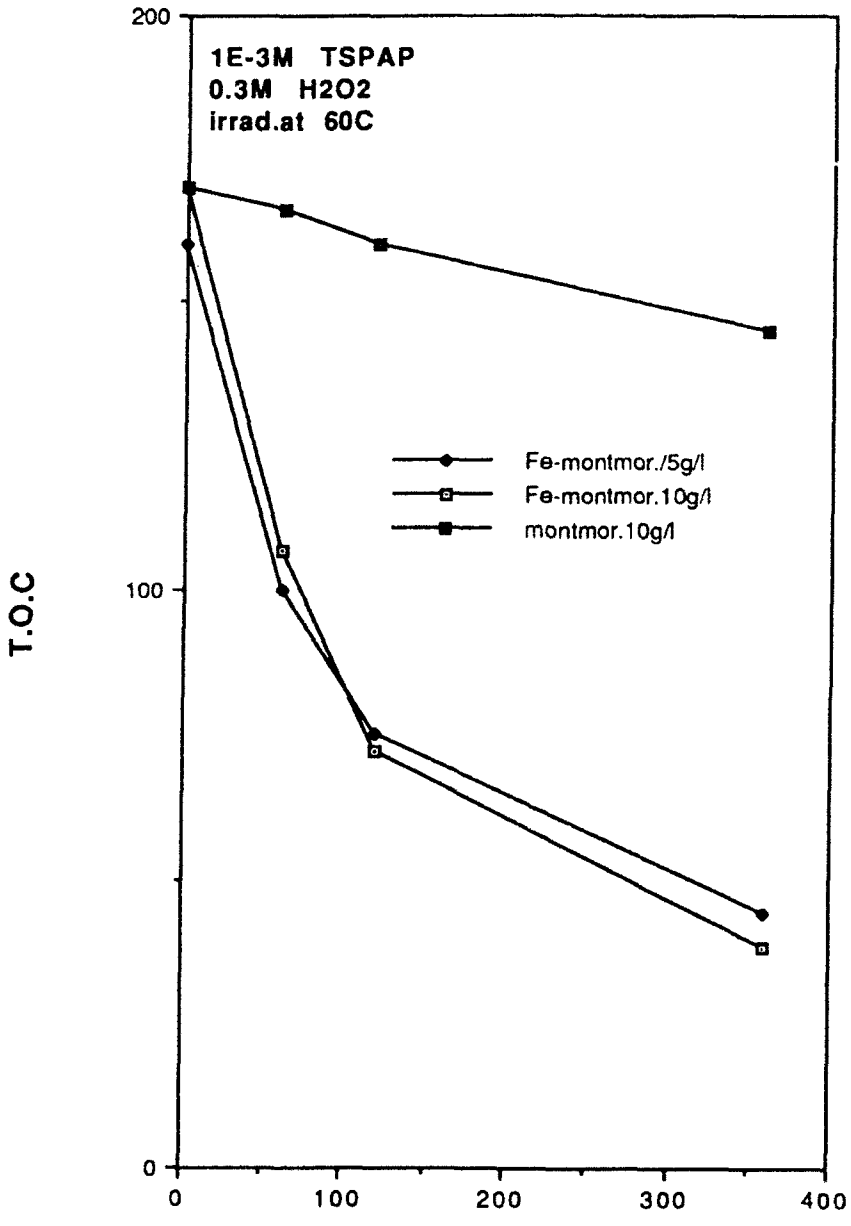

FIGURE 20